SIXTH INTERNATIONAL CONFERENCE ON CONTROL, AUTOMATION, ROBOTICS AND VISION (ICARCV 2002)
2 – 5 December 2002, Marina Mandarin, Singapore

# Kinematics Analysis and Mechatronics System Design Of a 3-DOF In-Parallel Actuated Mechanism

**HUYNH Patrick, WOON Kok Meng, HO Tai Tong, KWEE Tiaw Joo**

NgeeAnn Polytechnic
School of Engineering
Mechanical Engineering Division
535 Clementi Road, 599489 Singapore

## Abstract

*The paper aims to analyze the kinematics of a three-degree-of-freedom (3-DOF) in-parallel actuated mechanism, which can be used as a wrist robotic device. Basic kinematic models are given. Due to symmetry in mechanism geometry, the input-output polynomial degree derived in position forward kinematics can be considerably reduced. By analyzing the relationship between the independent and dependent motion parameters, 3 by 3 Jacobian matrices can be obtained. This will enable further real time control of the mechanism. A prototype mechanism is designed and fabricated based on the kinematics analysis and the simulation result of workspace volume computation.*

**Key Words:** *Parallel Mechanism, Kinematics Design, Workspace Computation, Jacobian Matrices.*

## 1 Introduction

During the past few years, there has been an increasing demand in the field of precision engineering for fine motion of multi-degrees of freedom. This motivates the development of a new robotics application field, parallel mechanism in the Mechanical Engineering Division at NgeeAnn Polytechnic, Singapore. The choice of parallel structures for high precision applications is justified by numerous advantages:

- High stiffness and structural frequency.
- Precision.
- Mobility and compactness.
- Fixed actuators.
- Uniform distribution of the load.

However, the main disadvantage is a limited working space. The simplest way to cumulate precision and working volume consists in the utilization of a parallel manipulator combined with classic-serial robots, as the active wrist [1,2]. The parallel manipulator thus compensates the static errors of the sequential robot with serial structure. This principle is often described by the name "Macro-/mini-manipulator" [3].

Most researchers are concerned with kinematic properties of the general 6-DOF parallel platform architecture. The design of in-parallel actuated mechanisms with less than 6-DOF is less developed. In many respects, the paper focuses on design and fabrication of a 3-DOF linear type in-parallel actuated mechanism evolved from previous research studies [4-6] and experiences concerning parallel robotic platform manipulators at Stanford University, USA [1,7] and Mechanical Engineering Laboratory, Japan [8,9].

This type of parallel mechanism has the potential to produce high precision, a desirable attribute for a robot wrist. Hence, the ideal application of such special parallel mechanism is a micro-motion manipulator [2]. The major goals of this project supported by NgeeAnn Polytechnic are:

- Development of the technology for new generation of robot systems carrying out dexterous manipulation tasks.
- To train Mechanical Engineering staff and students in kinematics modeling and motion control of closed-loop chain mechanisms attracting more and more attention as a competent device for robotics and automation.
- To support research and promote interest and skill development in robot manipulator design and control issues.

In this paper, closed-form inverse and forward kinematics analyses, with Jacobian matrices are first developed for the 3-DOF in-parallel actuated mechanism under constrained equations determining the relationship between independent and dependent motion parameters. Roth et al. in [1] had found in their general study on this mechanism, an input-output polynomial of degree 24, which seems to be difficult for real time control. Through detailed forward kinematics analysis and because of symmetric arrangement of the three base revolute joints, an important result shows that the input-output polynomial degree of the system can be considerably reduced, and hence minimize computational effort. Next, the mechanical design is described based on simulation result of workspace volume computation using a numerical procedure on inverse kinematics. Finally, some details of hardware implementation for further motion control development are presented with kinematic specification of the prototype.

## 2 Kinematics Analysis of a 3-DOF In-Parallel Actuated Mechanism

### 2.1 Kinematic Configuration

The prototype is a linear type 3-DOF parallel manipulator represented in Fig. 1. Its top view at initial position is illustrated in Fig. 2. It composed a mobile platform end-effector and a fixed base plate, connected by three variable length links. Each of the three serial links is coupled to a base plate through a passive revolute joint, and to the end-effector attachment plate through a nut, rotating freely about three perpendicular axes by virtue of a spherical joint coupling. Since the manipulator in this project is intended to be for general purpose, the base and mobile plates are both of equilateral triangle shape. The entire arrangement of attachment points on mobile and base plates is made as symmetric as possible to simplify analysis and operation.

This mechanism has three degrees of freedom: two for orientation (pitch and yaw rotations) and one for translation freedom (plunging motion), and can provide the necessary flexibility for insertion operations with accuracy. It is interesting to note that the axes of the orientation are changing according to the poses of the platform. Therefore, the two orientation degrees of freedom cannot be taken as rotational axes. But since the three base revolute joints are symmetrically arranged, the 2 fixed axes $x_0$ and $y_0$ as shown in Fig. 2 can be reasonably considered as orientation axes.

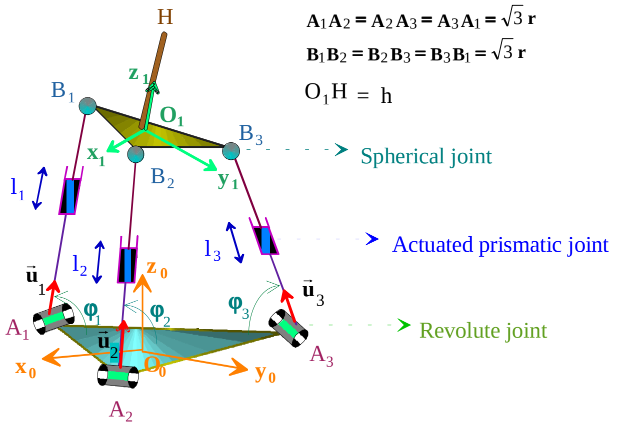


**Fig. 1:** *A linear type 3-DOF parallel mechanism*

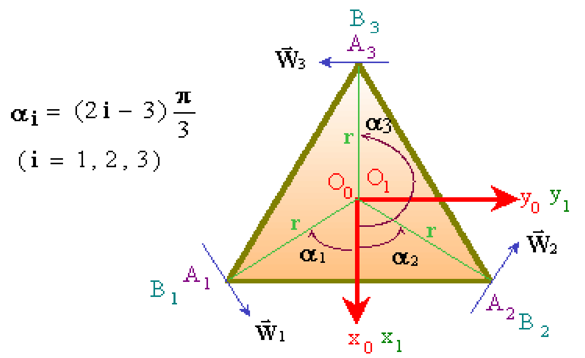


**Fig. 2:** *Top view at initial position*

## 2.2 Notations and Preliminary Results

Let $\mathfrak{R}_0$ a fixed coordinate frame ($\mathbf{O_0}$, $\vec{\mathbf{x}}_0$, $\vec{\mathbf{y}}_0$, $\vec{\mathbf{z}}_0$) attached to the center of base platform, $\mathfrak{R}_1$ a moving coordinate frame ($\mathbf{O_1}$, $\vec{\mathbf{x}}_1$, $\vec{\mathbf{y}}_1$, $\vec{\mathbf{z}}_1$) attached to center of the mobile platform, **r** radius from base center or from mobile platform center, $\alpha_i$ distribution angle **i** (**i** = 1,2,3) of base platform, $\varphi_i$ angle **i** (**i** = 1,2,3) from the median of base triangle to the linear link axis **i**, $\mathbf{l_i}$ length of the linear variable link **i** (**i** = 1,2,3) which is the controlled variable, **h** length of the end effector $\mathbf{O_1H}$, and $\mathbf{M}_{\mathfrak{R}_0}^{\mathfrak{R}_1}$ the transformation matrix between frame $\mathfrak{R}_0$ and frame $\mathfrak{R}_1$. Because only three among the six position and orientation parameters of mobile platform are independent, the end effector point **H** attached to mobile platform can be located either by the orientation angles ($\theta_X$, $\theta_Y$) which are pitch and yaw rotations, and the plunge distance **z** = $\mathbf{O_0O_1}$, or simply by the end effector position (**X**, **Y**, **Z**) of the point **H** expressed in the reference frame $\mathfrak{R}_0$.

Referring to Fig. 1 and Fig. 2, the unit vectors $\vec{\mathbf{u}}_i$ and $\vec{\mathbf{w}}_i$ in the reference frame $\mathfrak{R}_0$, the positions of points $\mathbf{O_1}$ and $\mathbf{A_i}$ (**i** = 1,2,3) in $\mathfrak{R}_0$, the positions of points $\mathbf{B_i}$ (**i** = 1,2,3) and **H** in the moving frame $\mathfrak{R}_1$ and the matrix $\mathbf{M}_{\mathfrak{R}_0}^{\mathfrak{R}_1}$ can respectively be expressed as follows:

$$\left(\vec{u}_i\right)_{\mathfrak{R}_0} = \begin{bmatrix} -\cos\alpha_i\cos\varphi_i \\ -\sin\alpha_i\cos\varphi_i \\ \sin\varphi_i \end{bmatrix}, \qquad \left(\vec{w}_i\right)_{\mathfrak{R}_0} = \begin{bmatrix} -\sin\alpha_i \\ \cos\alpha_i \\ 0 \end{bmatrix},$$

$$\left(\overrightarrow{O_0O_1}\right)_{\mathfrak{R}_0} = \begin{bmatrix} 0 \\ 0 \\ z \end{bmatrix}, \qquad \left(\overrightarrow{O_0A_i}\right)_{\mathfrak{R}_0} = \begin{bmatrix} r\cos\alpha_i \\ r\sin\alpha_i \\ 0 \end{bmatrix},$$

$$\left(\overrightarrow{O_1B_i}\right)_{\mathfrak{R}_1} = \begin{bmatrix} r\cos\alpha_i \\ r\sin\alpha_i \\ 0 \end{bmatrix}, \qquad \left(\overrightarrow{O_1H}\right)_{\mathfrak{R}_1} = \begin{bmatrix} 0 \\ 0 \\ h \end{bmatrix},$$

$$\mathbf{M}_{\mathfrak{R}_0}^{\mathfrak{R}_1} = \begin{bmatrix} \vec{x}_0\cdot\vec{x}_1 & \vec{x}_0\cdot\vec{y}_1 & \vec{x}_0\cdot\vec{z}_1 \\ \vec{y}_0\cdot\vec{x}_1 & \vec{y}_0\cdot\vec{y}_1 & \vec{y}_0\cdot\vec{z}_1 \\ \vec{z}_0\cdot\vec{x}_1 & \vec{z}_0\cdot\vec{y}_1 & \vec{z}_0\cdot\vec{z}_1 \end{bmatrix} = \begin{bmatrix} m_{11} & m_{12} & m_{13} \\ m_{21} & m_{22} & m_{23} \\ m_{31} & m_{32} & m_{33} \end{bmatrix}. \quad (1)$$

Using the pitch and yaw rotations ($\theta_X$, $\theta_Y$), $\mathbf{M}_{\mathfrak{R}_0}^{\mathfrak{R}_1}$ can be also written as

$$\mathbf{M}_{\mathfrak{R}_0}^{\mathfrak{R}_1} = \begin{bmatrix} \cos\theta_Y & 0 & \sin\theta_Y \\ 0 & 1 & 0 \\ -\sin\theta_Y & 0 & \cos\theta_Y \end{bmatrix} . \begin{bmatrix} 1 & 0 & 0 \\ 0 & \cos\theta_X & -\sin\theta_X \\ 0 & \sin\theta_X & \cos\theta_X \end{bmatrix}$$

$$= \begin{bmatrix} \cos\theta_Y & \sin\theta_X\sin\theta_Y & \cos\theta_X\sin\theta_Y \\ 0 & \cos\theta_X & -\sin\theta_X \\ -\sin\theta_Y & \sin\theta_X\cos\theta_Y & \cos\theta_X\cos\theta_Y \end{bmatrix}. \quad (2)$$

By identification, equations **(1)** and **(2)** yield

$$m_{11} = \cos\theta_Y, \quad m_{12} = \sin\theta_X\sin\theta_Y, \quad m_{13} = \cos\theta_X\sin\theta_Y. \quad (3)$$

$$m_{21} = 0, \quad m_{22} = \cos\theta_X, \quad m_{23} = -\sin\theta_X. \quad (4)$$

$$m_{31} = -\sin\theta_Y, \quad m_{32} = \sin\theta_X\cos\theta_Y, \quad m_{33} = \cos\theta_X\cos\theta_Y. \quad (5)$$

The position of the point **H** can be expressed in $\mathfrak{R}_0$ as

$$\left(\overrightarrow{O_0H}\right)_{\mathfrak{R}_0} = \begin{bmatrix} X \\ Y \\ Z \end{bmatrix} = \left(\overrightarrow{O_0O_1}\right)_{\mathfrak{R}_0} + \left(\overrightarrow{O_1H}\right)_{\mathfrak{R}_0}$$

$$= \begin{bmatrix} 0 \\ 0 \\ z \end{bmatrix} + \mathbf{M}_{\mathfrak{R}_0}^{\mathfrak{R}_1} . \begin{bmatrix} 0 \\ 0 \\ h \end{bmatrix} = \begin{bmatrix} m_{13}h \\ m_{23}h \\ z + m_{33}h \end{bmatrix}. \quad (6)$$

Equations **(3)**, **(4)**, **(5)** and **(6)** yield

$$\begin{bmatrix} X \\ Y \\ Z \end{bmatrix} = \begin{bmatrix} h\cos\theta_X\sin\theta_Y \\ -h\sin\theta_X \\ z + h\cos\theta_X\cos\theta_Y \end{bmatrix}. \quad (7)$$

Conversely, with $\theta_X \neq \frac{\pi}{2}$ equation **(7)** yields

$$\begin{bmatrix} \theta_X \\ \theta_Y \\ z \end{bmatrix} = \begin{bmatrix} -\sin^{-1}\left(\dfrac{Y}{h}\right) \\ \sin^{-1}\left(\dfrac{X}{h\cos\theta_X}\right) \\ Z - h\cos\theta_X\cos\theta_Y \end{bmatrix}. \quad (8)$$

Equations **(7)** and **(8)** express a dependent relationship between (**z**, $\theta_X$, $\theta_Y$) and (**X**, **Y**, **Z**).

The position of the point $\mathbf{O_1}$ can be expressed in $\mathfrak{R}_0$ as

$$\left(\overrightarrow{O_0O_1}\right)_{\mathfrak{R}_0} = \begin{bmatrix} 0 \\ 0 \\ z \end{bmatrix} = \frac{1}{3}\left(\overrightarrow{A_iB_i}\right)_{\mathfrak{R}_0} = \frac{1}{3}\sum_{i=1}^{3}\left(l_i\vec{u}_i\right)_{\mathfrak{R}_0} = \begin{bmatrix} -\frac{1}{3}\sum_{i=1}^{3} l_i\cos\alpha_i\cos\varphi_i \\ -\frac{1}{3}\sum_{i=1}^{3} l_i\sin\alpha_i\cos\varphi_i \\ \frac{1}{3}\sum_{i=1}^{3} l_i\sin\varphi_i \end{bmatrix}. \quad (9)$$

Equation **(9)** implies

$$\begin{cases} \sum_{i=1}^{3} l_i \cos\alpha_i \cos\varphi_i = \sum_{i=1}^{3} l_i \sin\alpha_i \cos\varphi_i = 0, & (10) \\ z = \frac{1}{3}\sum_{i=1}^{3} l_i \sin\varphi_i . & (11) \end{cases}$$

### 2.3 Inverse Kinematics

Inverse kinematics of this parallel mechanism are straightforward and can be stated as follows: *given a desired end effector orientation* ($\theta_X$ , $\theta_Y$ ) *and plunge distance* $z$*, or simply given a desired end effector position* (**X**, **Y**, **Z**)*, find a set of input lengths of the linear variable links* $l_i$ (**i** = 1,2,3), *producing the desired results.*

Writing from previous results:

$$l_i \vec{u}_i = \overrightarrow{A_i B_i} = \left(\overrightarrow{O_0 H}\right)_{\Re_0} - \left(\overrightarrow{O_0 A_i}\right)_{\Re_0} + \left(\overrightarrow{O_1 B_i}\right)_{\Re_0} + \left(\overrightarrow{O_1 H}\right)_{\Re_0}$$

$$= \begin{bmatrix} X - r\cos\alpha_i + m_{11} r\cos\alpha_i + m_{12} r\sin\alpha_i - m_{12} h \\ Y - r\sin\alpha_i + m_{21} r\cos\alpha_i + m_{22} r\sin\alpha_i - m_{23} h \\ Z + m_{31} r\cos\alpha_i + m_{32} r\sin\alpha_i - m_{33} h \end{bmatrix}. \qquad (12)$$

and taking the Euclidean norm of equation **(12)** for **i** = 1, 2, 3, one gets

$$l_i = \left\|\overrightarrow{A_i B_i}\right\| = \Big[\left(X - r\cos\alpha_i + m_{11} r\cos\alpha_i + m_{12} r\sin\alpha_i - m_{12} h\right)^2$$
$$+ \left(Y - r\sin\alpha_i + m_{21} r\cos\alpha_i + m_{22} r\sin\alpha_i - m_{23} h\right)^2$$
$$+ \left(Z + m_{31} r\cos\alpha_i + m_{32} r\sin\alpha_i - m_{33} h\right)^2\Big]^{1/2}.$$

From equations **(3)**, **(4)**, and **(5)**, coefficients $m_{ij}$ for **i** =1,2,3 and **j**= 1,2,3, are functions of ( $\theta_X$ , $\theta_Y$ ), hence from equation **(8)** they are also function of (**X**, **Y**).

### 2.4 Forward Kinematics

Forward kinematics of the proposed parallel manipulator are much more complicated and can be stated as follows: *given a set of input lengths of the linear variable links* $l_i$ (**i** = 1,2,3), *find the plunge distance* $z$ *and orientation* ( $\theta_X$ , $\theta_Y$ ) *of the tool coordinate frame, or simply find the end effector position* (**X**, **Y**, **Z**).

From previous notations and preliminary results, one can write for **i** = 1,2,3 and **j** = 1,2,3

$$\overrightarrow{B_i B_j} = -\left(\overrightarrow{O_0 A_i}\right)_{\Re_0} - \left(\overrightarrow{A_i B_i}\right)_{\Re_0} + \left(\overrightarrow{O_0 A_j}\right)_{\Re_0} + \left(\overrightarrow{A_i B_j}\right)_{\Re_0}$$

$$= \begin{bmatrix} -r\cos\alpha_i + l_i \cos\alpha_i \cos\varphi_i + r\cos\alpha_j - l_j \cos\alpha_j \cos\varphi_j \\ -r\sin\alpha_i + l_i \sin\alpha_i \cos\varphi_i + r\cos\alpha_j - l_j \sin\alpha_j \cos\varphi_j \\ -l_i \sin\varphi_i + l_j \sin\varphi_j \end{bmatrix}. \qquad (13)$$

Considering the equilateral triangle of mobile platform, one gets

$$\left\|\overrightarrow{B_i B_j}\right\|_{i \neq j}^2 = 3r^2 . \qquad (14)$$

Equations **(13)** and **(14)** give

$$l_i^2 + l_j^2 - 2 l_i l_j \sin\varphi_i \sin\varphi_j - 2r\, l_i \cos\varphi_i - 2r\, l_j \cos\varphi_j$$
$$+ \cos(\alpha_i - \alpha_j)\left[-2r^2 + 2r\, l_i \cos\varphi_i + 2r\, l_j \cos\varphi_j - 2 l_i l_j \cos\varphi_i \cos\varphi_j\right] = r^2 . \qquad (15)$$

With $\alpha_i - \alpha_j = (i - j)\frac{2\pi}{3}$ , $i \neq j$ , equation **(15)** yields

$$l_i^2 + l_j^2 + l_i l_j \cos\varphi_i \cos\varphi_j - 2 l_i l_j \sin\varphi_i \sin\varphi_j$$
$$- 3r\, l_i \cos\varphi_i - 3r\, l_j \cos\varphi_j = 0 . \qquad (16)$$

By permuting indices **i** and **j** in equation **(16)** the following system is obtained:

$$l_1^2 + l_2^2 + l_1 l_2 \cos\varphi_1 \cos\varphi_2 - 2 l_1 l_2 \sin\varphi_1 \sin\varphi_2 - 3r\, l_1 \cos\varphi_1 - 3r\, l_2 \cos\varphi_2 = 0 , \qquad (17)$$

$$l_2^2 + l_3^2 + l_2 l_3 \cos\varphi_2 \cos\varphi_3 - 2 l_2 l_3 \sin\varphi_2 \sin\varphi_3 - 3r\, l_2 \cos\varphi_2 - 3r\, l_3 \cos\varphi_3 = 0 , \qquad (18)$$

$$l_1^2 + l_3^2 + l_1 l_3 \cos\varphi_1 \cos\varphi_3 - 2 l_1 l_3 \sin\varphi_1 \sin\varphi_3 - 3r\, l_1 \cos\varphi_1 - 3r\, l_3 \cos\varphi_3 = 0 . \qquad (19)$$

to be solved for $\varphi_i$ (**i** = 1,2,3), given $l_i$ (**i** = 1,2,3). As stated by Roth et al. in [1], an input-output polynomial of degree 24 in $t_k$ (k=1,2,3) can be obtained by posing $t_k = \tan\left(\frac{\varphi_k}{2}\right)$, that means $\sin\varphi_k = \frac{2 t_k}{1 + t_k^2}$, $\cos\varphi_k = \frac{1 - t_k^2}{1 + t_k^2}$.

Once $t_k$ is found from input-output polynomial, $\varphi_k$ can be derived as $\varphi_k = 2\tan^{-1}(t_k)$.

In the following, the input-output polynomial degree is reduced by observing some simplified values of the coefficients $m_{ij}$ for **i** = 1,2,3 and **j** = 1,2,3, due to symmetry in mechanism geometry. Define the unit vectors $\vec{x}_1$ , $\vec{y}_1$ and $\vec{z}_1$ in $\Re_0$ as follows.

$$\vec{x}_1 = \frac{\overrightarrow{B_3 B_1} + \overrightarrow{B_3 B_2}}{\left\|\overrightarrow{B_3 B_1} + \overrightarrow{B_3 B_2}\right\|} \quad \text{with} \quad \left\|\overrightarrow{B_3 B_1} + \overrightarrow{B_3 B_2}\right\| = 3r ,$$

$$\vec{y}_1 = \frac{\overrightarrow{B_1 B_2}}{\left\|\overrightarrow{B_1 B_2}\right\|} \quad \text{with} \quad \left\|\overrightarrow{B_1 B_2}\right\| = \sqrt{3}\, r , \quad \vec{z}_1 = \vec{x}_1 \wedge \vec{y}_1 .$$

Using above results and from equation **(13)**, one obtains:

$$\left(\vec{x}_1\right)_{\Re_0} = \frac{1}{3r}\begin{bmatrix} 3r - \frac{l_1}{2}\cos\varphi_1 - \frac{l_2}{2}\cos\varphi_2 - 2 l_3 \cos\varphi_3 \\ \frac{\sqrt{3}}{2} l_1 \cos\varphi_1 - \frac{\sqrt{3}}{2} l_2 \cos\varphi_2 \\ l_1 \sin\varphi_1 + l_2 \sin\varphi_2 - 2 l_3 \sin\varphi_3 \end{bmatrix}.$$

By identification of coefficients $m_{ij}$ in equation **(1)**, we obtain $m_{ij}$ for **i** =1,2,3 and **j**= 1,2,3, in function of $(l_i, \varphi_i)_{(i=1,2,3)}$ . Particularly for $m_{21}$ one gets:

$$m_{21} = \vec{y}_0 . \vec{x}_1 = \frac{1}{2\sqrt{3}\, r}\left(l_1 \cos\varphi_1 - l_2 \cos\varphi_2\right). \qquad (20)$$

Since $m_{21} = 0$ , from equation **(4)** equation **(20)** implies

$$l_2 \cos\varphi_2 = l_1 \cos\varphi_1 . \qquad (21)$$

Difference between equations **(18)** and **(19)** yields

$$l_2^2 - l_1^2 - 2 l_3 \sin\varphi_3 (l_2 \sin\varphi_2 - l_1 \sin\varphi_1) = 0 . \qquad (22)$$

From equation **(21)**, arranging equation **(17)** yields

$$l_1^2 + l_2^2 + l_1^2 \cos^2\varphi_1 - 2 l_1 l_2 \sin\varphi_1 \sin\varphi_2 - 6r\, l_1 \cos\varphi_1 = 0 . \qquad (23)$$

Equation **(23)** implies

$$l_2 \sin\varphi_2 = \frac{l_1^2 + l_2^2 + l_1^2 \cos^2\varphi_1 - 6r\, l_1 \cos\varphi_1}{2 l_1 \sin\varphi_1} . \qquad (24)$$

Equation **(22)** implies

$$l_3 \sin\varphi_3 = \frac{l_2^2 - l_1^2}{2(l_2 \sin\varphi_2 - l_1 \sin\varphi_1)}$$
$$= \frac{(l_2^2 - l_1^2)\, l_1 \sin\varphi_1}{l_2^2 - l_1^2 + 3 l_1^2 \cos^2\varphi_1 - 6r\, l_1 \cos\varphi_1} . \qquad (25)$$

Squaring equations **(21)** and **(24)**, then their summation yields

$$l_2^2 = l_1^2 \cos^2\varphi_1 + \frac{\left(l_1^2 + l_2^2 + l_1^2 \cos^2\varphi_1 - 6r\, l_1 \cos\varphi_1\right)^2}{4 l_1^2 \sin^2\varphi_1} . \qquad (26)$$

With $\varphi_1 \neq k\pi$ , equation **(26)** yields

$$3l_1^4\cos^4\varphi_1 + 12r\,l_1^3\cos^3\varphi_1 - \left(6l_1^4 + 6l_1^2 l_2^2 + 36r^2 l_1^2\right)\cos^2\varphi_1$$
$$+12\left(l_1^2 + l_2^2\right)r\,l_1\cos\varphi_1 - \left(l_1^2 - l_2^2\right)^2 = 0. \quad \textbf{(27)}$$

Posing $\mathbf{t} = \cos\varphi_1$, equation **(27)** implies

$$3l_1^4 t^4 + 12r\,l_1^3 t^3 - \left(6l_1^4 + 6l_1^2 l_2^2 + 36r^2 l_1^2\right)t^2$$
$$+12\left(l_1^2 + l_2^2\right)r\,l_1 t - \left(l_1^2 - l_2^2\right)^2 = 0. \quad \textbf{(28)}$$

The input-output polynomial degree in **t** is now only 4. Once **t** is determined from equation **(28)**, $\varphi_1 = \cos^{-1}(t)$. Equation **(23)** yields $\varphi_2 = \sin^{-1}\left(\dfrac{l_1^2 + l_2^2 + l_1^2 t^2 - 6r\,l_1 t}{2l_1 l_2 \sin\varphi_1}\right)$. Finally, equation **(25)** yields $\varphi_3 = \sin^{-1}\left(\dfrac{(l_2^2 - l_1^2)\,l_1 \sin\varphi_1}{l_3(l_2^2 - l_1^2 + 3l_1^2 t^2 - 6r\,l_1 t)}\right)$.

So, when angles $\varphi_i$ (**i** = 1,2,3) are known for given $l_i$, the end effector position (**X**, **Y**, **Z**) of the point **H** can be determined through equations **(6)** and **(11)**.

### 2.5 Jacobian Matrices

Let $\vec{p} = \overrightarrow{O_0H}$, $\vec{p}_{A_i} = \overrightarrow{O_0A_i}$, and $\vec{S}_i = \overrightarrow{HB_i} = \overrightarrow{O_1B_i} - \overrightarrow{O_1H}$.

From the relation $l_i\vec{u}_i = \overrightarrow{A_iB_i} = \overrightarrow{A_iO_0} + \overrightarrow{O_0H} + \overrightarrow{HO_1} + \overrightarrow{O_1B_i}$, one can write

$$l_i\vec{u}_i = \vec{p} + \vec{S}_i - \vec{p}_{A_i}. \quad \textbf{(29)}$$

Differentiating equation **(29)** with respect to time domain yields

$$\dot{l}_i\vec{u}_i + l_i\dot{\vec{u}}_i = \dot{\vec{p}} + \dot{\vec{S}}_i. \quad \textbf{(30)}$$

With $\dot{\vec{p}} = \vec{V}$ and $\dot{\vec{S}}_i = \vec{\Omega}\wedge\vec{S}_i$, where $\vec{V}$ is the translational velocity of point **H** and $\vec{\Omega}$ is the angular velocity of mobile platform, equation **(30)** yields

$$\dot{l}_i\vec{u}_i + l_i\dot{\vec{u}}_i = \vec{V} + \vec{\Omega}\wedge\vec{S}_i. \quad \textbf{(31)}$$

Multiplying equation **(31)** by the unit vector $\vec{u}_i$ yields

$$\dot{l}_i = \vec{V}.\vec{u}_i + \left(\vec{\Omega}\wedge\vec{S}_i\right).\vec{u}_i. \quad \textbf{(32)}$$

By using the following property of cross and inner products of vectors $\left(\vec{a}\wedge\vec{b}\right)\cdot\vec{c} = \left(\vec{b}\wedge\vec{c}\right)\cdot\vec{a}$, one gets in matrix form

$$\dot{l}_i = \vec{u}_i.\vec{V} + \left(\vec{S}_i\wedge\vec{u}_i\right).\vec{\Omega} = \begin{bmatrix}\vec{u}_i^T & \vec{S}_{U_i}^T\end{bmatrix}\begin{bmatrix}\vec{V}\\ \vec{\Omega}\end{bmatrix}, \quad \textbf{(33)}$$

where $\vec{u}_i^T$ is the transpose of $\vec{u}_i$ and $\vec{S}_{U_i}^T = \left(\vec{S}_i\wedge\vec{u}_i\right)^T$.

Equation **(33)** yields $\dot{\vec{l}} = \begin{bmatrix}\dot{l}_1\\ \dot{l}_2\\ \dot{l}_3\end{bmatrix} = [U].\vec{V} + [S_U].\vec{\Omega}$, **(34)**

where

$$[U] = [\vec{u}_1 \quad \vec{u}_2 \quad \vec{u}_3]^T,\ [S_U] = [\vec{S}_1\wedge\vec{u}_1 \quad \vec{S}_2\wedge\vec{u}_2 \quad \vec{S}_3\wedge\vec{u}_3]^T.$$

The actuator velocity $\dot{\vec{l}}$ obtained from equation Eq.33 will not necessary produce the given translational velocity $\vec{V}$ and the angular velocity $\vec{\Omega}$ of mobile platform. This is due to the fact that the mobile platform has only 3 motion parameters out of six which are independent, therefore further constraint equations are needed to form the relationship between independent and dependent velocity parameters.

Since $\vec{w}_i.\vec{u}_i = \vec{w}_i.\dot{\vec{u}}_i = 0$, multiplying equation **(31)** by the unit vector $\vec{w}_i$ yields

$$\vec{V}.\vec{w}_i + \left(\vec{\Omega}\wedge\vec{S}_i\right).\vec{w}_i = 0. \quad \textbf{(35)}$$

Arranging equation **(35)** yields

$$\vec{V}.\vec{w}_i = -\left(\vec{\Omega}\wedge\vec{S}_i\right).\vec{w}_i = -\left(\vec{S}_i\wedge\vec{w}_i\right).\vec{\Omega}.$$

In matrix form, this can be written

$$[W]\vec{V} = [S_W]\vec{\Omega}, \quad \textbf{(36)}$$

with

$$[W] = [\vec{w}_1 \quad \vec{w}_2 \quad \vec{w}_3]^T,\ [S_W] = [-\vec{S}_1\wedge\vec{w}_1 \quad -\vec{S}_2\wedge\vec{w}_2 \quad -\vec{S}_3\wedge\vec{w}_3]^T.$$

If matrices [**W**] and [$S_W$] are non-singular, one gets from equation **(36)**: $\vec{V} = [W]^{-1}.[S_W].\vec{\Omega}$, **(37)**

or $\vec{\Omega} = [S_W]^{-1}.[W].\vec{V}$. **(38)**

Equations **(34)**, **(37)** and **(38)** yield

$$\dot{\vec{l}} = \begin{bmatrix}\dot{l}_1\\ \dot{l}_2\\ \dot{l}_3\end{bmatrix} = \left([U] + [S_U].\left([S_W]^{-1}.[W]\right)\right).\vec{V} = \left([U].\left([W]^{-1}.[S_W]\right) + [S_U]\right).\vec{\Omega} \quad \textbf{(39)}$$

Equation **(36)** indicates that three components of the velocity $\vec{V}$ are independent parameters, as soon as $\vec{V}$ is given, the actuator velocity $\dot{\vec{l}}$ and angular velocity $\vec{\Omega}$ will be determined. Similarly, three components of the angular velocity $\vec{\Omega}$ can be considered as independent parameters, as soon as $\vec{\Omega}$ is given, $\dot{\vec{l}}$ and $\vec{V}$ will be determined.

Posing $J_V = [U] + [S_U].\left([S_W]^{-1}.[W]\right)$,

and $J_\Omega = [U].\left([W]^{-1}.[S_W]\right) + [S_U]$,

$J_V$ and $J_\Omega$ are 3 by 3 square Jacobian matrices of the parallel mechanism. They represent the mapping between the input rates and the independent output parameters, and will take different forms when different independent parameters are specified.

## 3 Mechanical System Design

Our design objective is to obtain the smallest size of the mechanism based on kinematics analysis and commercially available mini-motors. Based on inverse kinematics, the workspace volume can be estimated by limiting the motion range of actuators $(l_i, \varphi_i)_{(i=1,2,3)}$. One of the most interesting point in this mechanism design is to select a value **ρ**, representing the ratio between the length of equilateral triangle of end plate $a_1$ and that of the fixed base plate $a_0$, which produces a large workspace volume. Based on available size of mini-motors, the minimum value of $a_0$ is 89mm. The case **ρ** > 1 is excluded, because end plate inertia will be higher than the one of base plate, and therefore the dynamic performance characteristics such as high speed and acceleration cannot be obtained. First the volume is estimated by limiting the actuator motion range $l_i$ (**i** = 1,2,3), and then the volume is refined by taking into account the motion range of the pin joints $\varphi_i$ (**i** = 1,2,3) (for pin joint **i**, $55^\circ \le \varphi_i \le 90^\circ$).

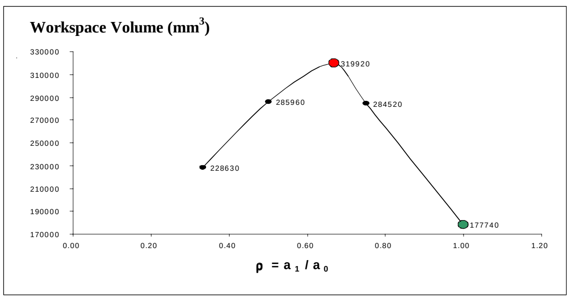


**Fig. 3:** *Computed workspace volume as a function of* **ρ**

Based on simulation result illustrated in Fig. 3, one can notice that the workspace volume is gradually increasing with the ratio $\rho$ until it reaches its maximum point corresponding to $\rho = 2/3$. Beyond this point, the workspace volume is gradually decreasing. To design a parallel manipulator with a different size of mobile and base platforms in the sense of achieving largest workspace, the 2/3 ratio offers the best performance.

It has been stated in [5] that as $\rho$ increases the force sensing ability of the parallel mechanism increases. So, to compromise the force sensing and force acting capabilities of the parallel mechanism, it was decided that $\rho$ would be unity. Another benefit of choosing $\rho$ as 1 is that the individual contribution of each actuator to end plate motion is decoupled, so the kinematics analysis are simplified as much as possible, and therefore the mechanism can be used for real time control.

A prototype parallel mechanism illustrated in Fig. 4 has been designed using Pro-Engineer software, and CNC machined for educational purpose at the Mechanical Engineering Division of the NgeeAnn Polytechnic of Singapore. The 3D workspace of the parallel manipulator when $\rho = 1$, is plotted in Fig. 5 by a numerical procedure explained in [10].

## 4 Hardware Implementation

The outline of the hardware system is shown in Fig. 6. Table 1 summarizes the kinematic specification of the proposed 3-DOF parallel mechanism. The whole system consists of 5 subsystems, which are a parallel mechanism, an actuators system, a sensors system, a controller, and a task environment. The components of those subsystems are described below.

### 4.1 Parallel Mechanism

The three actuated prismatic joints are based on ball-screw system. Each of the three ball-screws is coupled to a base plate through a passive revolute joint, and to the end-effector attachment plate through a nut which is free to rotate about three perpendicular axes by virtue of a spherical joint coupling, which is customized using the THK spherical plain bearing type SA1 from Japan.

### 4.2 Actuators System

The linear actuator is obtained from the combination of an electric motor and a ball-screw system. Each link is driven by a DC-servomotor 2036U giving a peak rated torque about 0.22[Nm]. The choice of those actuator characteristics is based on the requirement for end effector load capacity of about 30N.

### 4.3 Sensors System

For each link an incremental rotary 5[V] DC encoder with 2500ppr resolution is connected directly to the bottom of each motor to measure the linear displacement of the link. In addition, a joint encoder is mounted on the trunnion axis at the lower end of each of the three links. Totally, there are 3 encoders providing the necessary data for the control loop and 3 joint encoders for forward kinematics solution. Also, 3 proximity sensors are mounted on the parallel mechanism to make sure that the mobile platform can find its home position. An opto-coupler circuit TLP521-4 is used to protect and isolate control signals between the proximity sensors and the motion controller kit.

### 4.4 Controller

The parallel manipulator can be controlled entirely by software run on an IBM PC Pentium III computer with an input-output (I/O) expansion unit. This PC computer is used as a user interface and for real time determination of the control input. The control system is based on the conventional PID scheme used for low-level position servos of the three DC motors. The computation required for the control is only inverse kinematics, which is very simple for the parallel-link manipulators. The motion is generated by preplanned motion data.

Data measured from the two F/T sensors are input through two F/T receiver cards model JR3 DSP plugged into 16 bit on the PC ISA bus.

Pulses from the three incremental encoders representing 3 joint positions are input into counter circuit through a motion controller card from Motion Engineering, Inc. (MEI) which plugs into 16 bits on the PC ISA bus. The PC computer via the AT-bus lines reads the encoder pulses. A buffer circuit connects the 3 additional encoders representing 3 revolute joint angles installed on the pin joints at the base plate to an analog-digital A/D converter card model NuDaq-PCI8133. The PC computer performs calculations based on the control algorithm and generates signal to the digital-analog D/A converter built in the MEI card. The analog signals enter the three servo amplifiers model minimotor-BLD 5603/06, which produce output current proportional to the voltages of input signals. The currents generate motor torques to drive the mechanical links through the ball screws system. Further control software can be written in C language using Microsoft Visual C/C++ development package.

### 4.5 Task Environment

For insertion operation, a material of contact object containing a hole is fabricated and a tool (peg) is mounted at the end effector of the parallel manipulator. Both are made of steel. The peg and the hole are 20[mm] in diameter and the clearance is 10[μm]. Chamfer is less than 0.2[mm] in peg and hole. The insertion task may consist of 4 following motions:

- Approach the hole chamfer vertically using plunging motion.
- Move along the hole chamfer using pitch and yaw rotations.
- Align the peg to the hole axis.
- Insert by applying a constant speed along the hole axis.

## 5 Conclusion

In this paper, a detailed kinematics analysis of a 3-DOF in-actuated parallel mechanism showing a reduced input-output polynomial degree derived from position forward kinematics, and 3 by 3 square Jacobian matrices have been presented. This will support further works on the real time control of such mechanism with minimal computational effort.

Based on the simulation study of workspace volume using inverse kinematics, a prototype parallel mechanism has been designed and fabricated for educational purpose. The whole mechatronics system has been developed and described with its different subsystems.

Future R&D works will be carried out on the testing of the mechatronics system and the development of a macro-micro-manipulator using the above prototype parallel mechanism mounted on a serial articulated robot arm.

## Acknowledgments

The authors would like to acknowledge the financial support of NgeeAnn Polytechnic of Singapore, and wish to express their appreciation to the team of Automated Micron Assembly Pte Ltd for their machining works, to the technical support officers and final year students of Robotics and Automation Development programme for their useful assistance, and to Professor Michel Cotsaftis from LTME/ECE, France, for his fruitful discussions and comments on this paper.

## References

[1] B. Roth, K. J. Waldron, M. Raghavan, "Kinematics of a Hybrid Series-Parallel Manipulator System", ASME *Journal of Dynamic Systems, Measurement, and Control*, Vol.111, 1989, pp.211-221.

[2] C. Reboulet and R. Pigeyre, "Hybrid Control of a 6-DOF In-Parallel Actuated Micro-Manipulator mounted on a Scara Robot", *International Journal of Robotics and Automation*, Vol.7, No.1, 1992, pp.10-14.

[3] O. Khatib, "Reduced Effective Inertia in Macro-/Mini-Manipulator Systems", *Robotics Research 5*, Miura H. and Arimoto S., Eds., Cambridge: MIT press, 1990, pp.279-284.

[4] K. M. Lee and D. K. Shah, "Kinematic Analysis of a Three-Degrees-of-Freedom In-Parallel Actuated Manipulator", *Proceedings of the International Conference on Robotics and Automation*, Raleigh, USA, 1987, Vol.1, pp.345-350.

[5] George H. Pfeundshuh et al.: "Design and Control of 3-DOF In-Parallel Actuated Manipulator". *Proceedings of 1991 IEEE international conference on Robotics and Automation*, Sacramento, California, USA, April 1991.

[6] Y. Fang and Z. Huang, "Kinematics of a Three-Degree-of-Freedom In-Parallel Actuated Manipulator Mechanism", *Mechanism and Machine Theory*, Vol.32, No.7, pp.789-796, 1997.

[7] P. Huynh, "Dynamic Modeling of the ARTISAN Macro-/mini-Manipulator", *Postdoctoral report*, Stanford University, Dec. 1993.

[8] T. Arai et al., "Development of a New Parallel Manipulator with Fixed Linear Actuator", *Proceedings of the Japan-USA Symposium on Flexible Automation*, Boston, USA, July 7-10, 1996, pp.145-149.

[9] P. Huynh et al., "Optimal Velocity Based Control of a Parallel Manipulator with Fixed Linear Actuators", *Proceedings of the IEEE/RSJ International Conference on Intelligent Robot and Systems*, Grenoble, France, Sept. 7-11,1997, pp.1125-1130.

[10] P. Huynh, "Kinematic Performance Evaluation of Linear Type Parallel Mechanisms". *Sixth International Conference on Control, Automation, Robotics and Vision (ICARCV2000)*, Singapore, December 05 - 08, 2000.


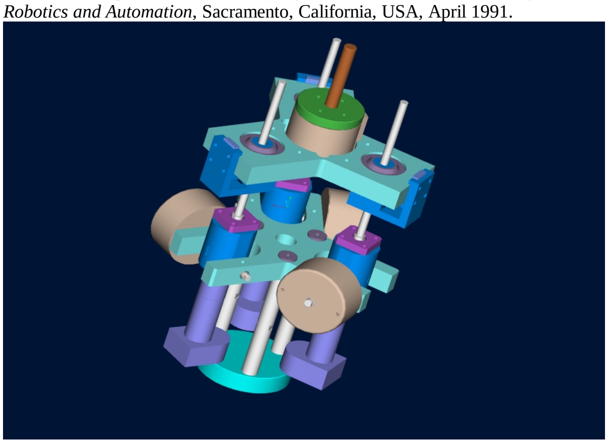

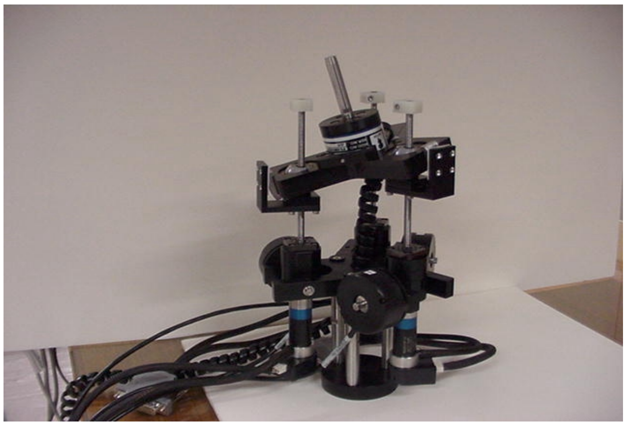

**Pro/E Design** **CNC Fabrication**

**Fig. 4:** *3-DOF in-parallel actuated mechanism*

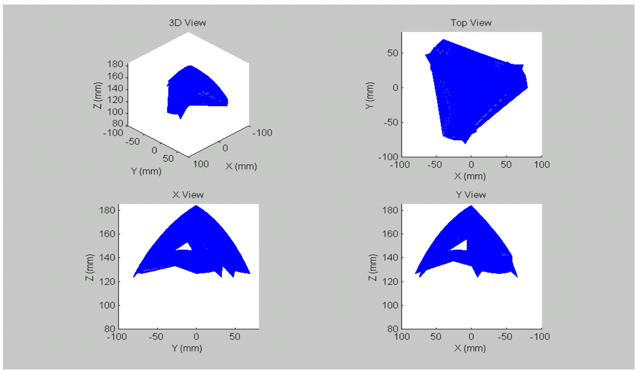


**Fig. 5:** *Workspace volume estimation*

| | Range | Units |
|---|---|---|
| Ball-screw stroke | Min: +25<br>Max: +64 | mm |
| Total length of ball-screw | 120 | mm |
| Pitch of ball-screw | 2 π | rad/mm |
| Length of equilateral triangle | 89 | mm |
| Height of tool center point | 90 | mm |
| Weight | 3 | kg |
| Load capacity | 3 | kg |
| DC motor output<br>Max. Torque | 0.5 | Nm |
| Encoder resolution | 2500 | ppr |
| Workspace volume | 0.2 | $dm^3$ |
| Resolution of motion: Z | 11 | μm |
| Resolution of motion: X, Y | 34 | μm |
| Velocity (max) of the end effector | 0.013 | m/s |

**Table 1:** *Specification of the prototype*

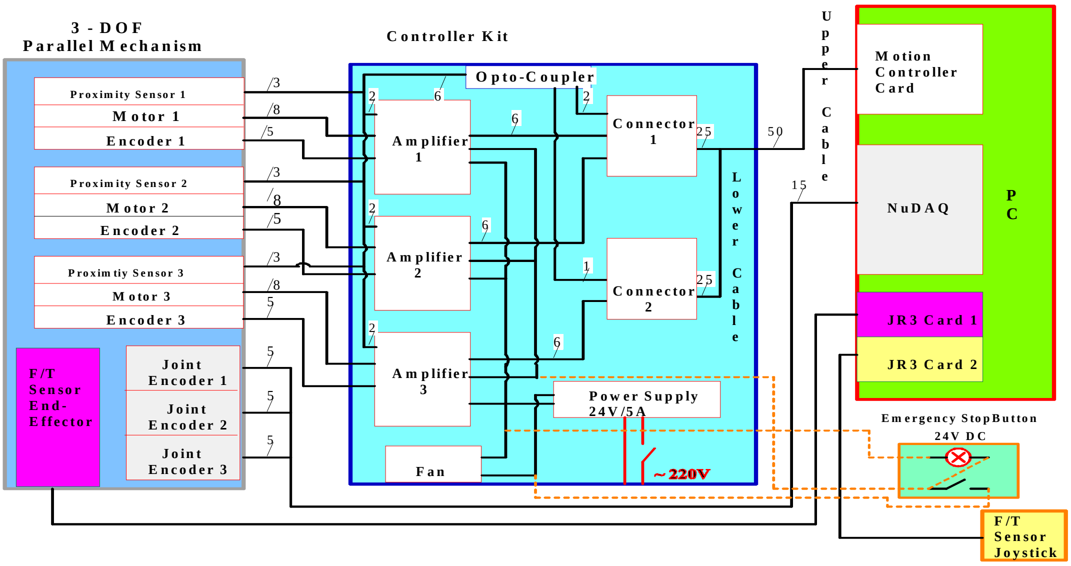


**Fig. 6:** *Mechatronics system control of the parallel mechanism*